7182 *Inorg. Chem.* **2010**, *49*, 7182–7187
DOI: 10.1021/ic101236x

Inorganic Chemistry
Article

Preparation, Crystal Structure, and Unusually Facile Redox Chemistry of a Macrocyclic Nitrosylrhodium Complex

Kathleen E. Kristian, Wenjing Song, Arkady Ellern, Ilia A. Guzei, and Andreja Bakac*

Ames Laboratory, Iowa State University, Ames, Iowa 50011

Received June 21, 2010

The reaction between NO and $L^2(H_2O)Rh^{2+}$ (L^2 = *meso*-Me_6-1,4,8,11-tetraazacyclotetradecane) generates a sky-blue $L^2(H_2O)RhNO^{2+}$, a $\{RhNO\}^8$ complex. The crystal structure of the perchlorate salt features a bent Rh−N−O moiety (122.1(11)°), short axial Rh−NO bond (1.998(12) Å) and a strongly elongated Rh−OH_2 (2.366(6) Å) trans to NO. Acidic aqueous solutions of $L^2(H_2O)RhNO^{2+}$ are stable for weeks, and are inert toward oxygen. The complex is oxidized rapidly and reversibly with $Ru(bpy)_3^{3+}$, $k_f = (1.9 \pm 0.1) \times 10^5$ M^{-1} s^{-1}, to an intermediate believed to be $L^2(H_2O)RhNO^{3+}$. This unprecedented $\{RhNO\}^7$ species has a lifetime of about 90 s at room temperature at pH 0. The reverse reaction between $L^2(H_2O)RhNO^{3+}$ and $Ru(bpy)_3^{2+}$ has $k_r = (1.5 \pm 0.4) \times 10^6$ M^{-1} s^{-1}. The kinetic data define the equilibrium constant for the $L^2(H_2O)RhNO^{2+}/Ru(bpy)_3^{3+}$ reaction, $K = k_f/k_r = 0.13$, and yield a reduction potential for the $L^2(H_2O)RhNO^{3+/2+}$ couple of 1.31 V. Both the redox thermodynamics of $L^2(H_2O)RhNO^{3+/2+}$ and the kinetics of the reactions with $Ru(bpy)_3^{3+/2+}$ are quite similar to those of uncoordinated NO^+/NO.

Introduction

Efforts geared toward an understanding of the complex roles that nitric oxide plays in biology have produced a number of novel nitrosylmetal complexes. Among various aspects of the chemistry of such complexes, the binding and release of nitric oxide, eq 1 (M = metal, L = ligand system) have received special attention.[1−8]

$$LM^n + NO \rightleftarrows LMNO^n \quad (1)$$

The reverse of reaction 1 sometimes provides a useful route to NO for chemical and medicinal purposes. The kinetics of this step are a sensitive function of the ligand system, solvent, pH, and the metal.[9,10] As one might expect, the oxidation state of the metal strongly influences the NO dissociation rates, so that the reduction[11] or oxidation[12,13] of inert nitrosyl complexes may provide a mechanism for NO release. In view of the complex electronic structure of nitrosyl complexes,[14] with three limiting (M^n-•NO, M^{n+1}-NO^-, and M^{n-1}-NO^+) and countless intermediate electronic states, the entire MNO moiety should be considered the site of electron transfer, as opposed to purely metal-centered or NO-centered processes. None the less, it is customary and often useful to assign discrete oxidation states to the metal and NO when discussing the chemistry of metal nitrosyl complexes.

In our earlier work,[12,13] we have examined the oxidation of nitrosylchromium complexes $Cr(H_2O)_5NO^{2+}$ and $L(H_2O)$-$CrNO^{2+}$ (L = L^1 = 1,4,8,11-tetraazacyclotetradecane, and L^2 = *meso*-Me_6-1,4,8,11-tetraazacyclotetradecane) with polypyridine complexes of iron(III) and ruthenium(III), $M(NN)_3^{3+}$. Four equivalents of $M(NN)_3^{3+}$ were required for complete oxidation which yielded nitrate and Cr(III). Detailed mechanistic studies supported an initial electron transfer to generate a one-electron oxidized nitrosyl complex followed by rapid dissociation of NO, as shown for $Cr(H_2O)_5NO^{2+}$ in eqs 1−3. The follow-up chemistry consumed three more equivalents of $M(NN)_3^{3+}$, as in eq 4, resulting in the observed stoichiometry and products.

$$Cr(H_2O)_5NO^{2+} + M(NN)_3^{3+} \longrightarrow Cr(H_2O)_5NO^{3+} + M(NN)_3^{2+} \quad (2)$$

*To whom correspondence should be addressed. E-mail: bakac@ameslab.gov.

(1) Ford, P. C. *Acc. Chem. Res.* **2008**, *41*, 190–200.
(2) Ford, P. C.; Lorkovic, I. M. *Chem. Rev.* **2002**, *102*, 993–1017.
(3) Ford, P. C.; Bourassa, J.; Miranda, K.; Lee, B.; Lorkovic, I.; Boggs, S.; Kudo, S.; Laverman, L. *Coord. Chem. Rev.* **1998**, *171*, 185–202.
(4) Haas, K. L.; Franz, K. *J. Chem. Rev.* **2009**, *109*, 4921–4960.
(5) Eroy-Reveles, A. A.; Leung, Y.; Beavers, C. M.; Olmstead, M. M.; Mascharak, P. K. *J. Am. Chem. Soc.* **2008**, *130*, 4447–4458.
(6) McCleverty, J. A. *Chem. Rev.* **2004**, *104*, 403–418.
(7) Hayton, T. W.; Legzdins, P.; Sharp, W. B. *Chem. Rev.* **2002**, *102*, 935–991.
(8) Moller, J. K. S.; Skibsted, L. H. *Chem. Rev.* **2002**, *102*, 1167–1178.
(9) Wanat, A.; Wolak, M.; Orzel, L.; Brindell, M.; van Eldik, R.; Stochel, G. *Coord. Chem. Rev.* **2002**, *229*, 37–49.
(10) Works, C. F.; Jocher, C. J.; Bart, G. D.; Bu, X.; Ford, P. C. *Inorg. Chem.* **2002**, *41*, 3728–3739.
(11) Lang, D. R.; Davis, J. A.; Lopes, L. G. F.; Ferro, A. A.; Vasconcellos, L. C. G.; Franco, D. W.; Tfouni, E.; Wieraszko, A.; Clarke, M. J. *Inorg. Chem.* **2000**, *39*, 2294–2300.
(12) Song, W.; Bakac, A. *Chem.—Eur. J.* **2008**, *14*, 4906–4912.
(13) Song, W.; Ellern, A.; Bakac, A. *Inorg. Chem.* **2008**, *47*, 8405–8411.
(14) Roncaroli, F.; Videla, M.; Slep, L. D.; Olabe, J. A. *Coord. Chem. Rev.* **2007**, *251*, 1903–1930.

Published on Web 07/06/2010

$$Cr(H_2O)_5NO^{3+} \xrightarrow{H_2O,\ fast} Cr(H_2O)_6{}^{3+} + NO \qquad (3)$$

$$NO + 3M(NN)_3{}^{3+} + 2H_2O \longrightarrow NO_3{}^- + 3M(NN)_3{}^{2+} + 4H^+ \qquad (4)$$

The reactions shown in eqs 1−3 parallel the oxidation of superoxochromium complexes $Cr(H_2O)_5OO^{2+}$ and $L(H_2O)$-$CrOO^{2+}$, which yielded Cr(III) and O_2 as in eqs 5a and 5b.

$$Cr(H_2O)_5OO^{2+} + M(NN)_3{}^{3+} \xrightarrow{-M(NN)_3{}^{2+}} [Cr(H_2O)_5OO^{3+}] \qquad (5a)$$

$$[Cr(H_2O)_5OO^{3+}] \xrightarrow{fast,\ H_2O} Cr(H_2O)_6{}^{3+} + O_2 \qquad (5b)$$

In none of the reactions examined was the product of the initial electron transfer, $LCrNO^{3+}$ or $LCrOO^{3+}$ (L = $(H_2O)_5$, L^1, or L^2), detected spectroscopically or kinetically. All the evidence suggested that the homolysis to LCr(III) and NO (or O_2) was extremely fast and essentially complete on the same time scale as the oxidations in eq 1 (or 5a).

The ready loss of NO from the oxidized Cr(III) nitrosyl complexes is not unexpected in view of their electronic structure, $\{CrNO\}^4$ in Enemark-Feltham notation.[15] In contrast, the more electron-rich nitrosyl complexes, such as those of iron and ruthenium, exist in both reduced and oxidized forms, that is, $\{MNO\}^7$ and $\{MNO\}^6$.[14,16,17] We reasoned that oxidation of even more electron-rich, late transition metal nitrosyls might provide a route to compounds that could not be generated by traditional means such as direct substitution by NO at the oxidized metal center. If successful, this approach could provide a new source of metal nitrosyls and new insights into their chemistry. This hypothesis was tested by synthesizing a novel rhodium nitrosyl complex, $L^2(H_2O)Rh^{III}NO^{2+}$, and exploring its reaction with $Ru(bpy)_3{}^{3+}$ in search of a $\{RhNO\}^7$ complex, for which, to the best of our knowledge, there is no precedent. The ligand L^2 is the same as that used in some of our earlier work with chromium to make the comparison between the metals as straightforward as possible.

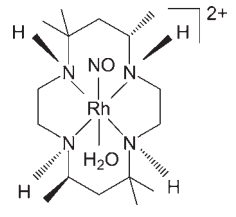

$L^2(H_2O)RhNO^{2+}$

Experimental Section

Solutions of $L^2(H_2O)Rh^{2+}$ were generated by 313-nm photolysis (Luzchem LZC-5 Reactor) of $L^2(H_2O)RhH^{2+}$ under argon. Gaseous NO (Matheson) was purified by passage through Ascarite, sodium hydroxide, and water. Stock solutions of NO prepared by bubbling the purified gas through argon-saturated 0.10 M $HClO_4$ for 30 min contained 1.7 mM NO and about 0.2 mM nitrous acid.[18] Solutions of $Ru(bpy)_3{}^{3+}$ were generated photochemically from $Ru(bpy)_3{}^{2+}$ and excess $(NH_3)_5Co(H_2O)^{3+}$ (2 mM).[19] In-house distilled water was further purified by passage through a Barnstead EASY pure III system. Deuterated solvents were obtained from Cambridge Isotopes and used as received. The concentration of nitrate generated from $L^2(H_2O)RhNO^{2+}$ and excess $Ru(bpy)_3{}^{3+}$ was determined spectrophotometrically (λ_{max} 200 nm, $\varepsilon = 1.0 \times 10^4$ M^{-1} cm^{-1}) after the passage of the sample through a short column of Dowex 50W X2 cation exchange resin to remove metal cations.

$[L^2(H_2O)RhNO](OTf)_2$ (MW 733.55) was prepared by bubbling NO through acidic (5−10 mM CF_3SO_3H) solutions of $L^2(H_2O)Rh^{2+}$, yielding pale-blue solutions. Evaporation under argon produced blue crystals. Anal. Calcd for $C_{18}H_{38}N_5O_8F_6S_2Rh$: C, 29.47; H, 5.22; N, 9.55; S, 8.74. Found: C, 29.88; H, 5.07; N, 9.70; S, 9.17. IR (photoacoustic, solid state): 1624, 1674 cm^{-1}, IR (aqueous solution, 0.01 M $HClO_4$):1651 cm^{-1}. UV−vis (0.01 M $HClO_4$): λ_{max} = 648 nm (broad, ε = 30 M^{-1} cm^{-1}); 370 nm (shoulder, ε = 78 M^{-1} cm^{-1}). ^1H NMR (400 MHz, 298 K, D_2O): δ 5.74 (br s, 1H, N*H*), 5.05 (br s, 1H, N*H*), 4.90 (br s, 1H, N*H*), 4.12 (br s, 1H, N*H*), 3.57−3.36 (m, 3H), 3.16−2.99 (m, 3H), 2.71−2.48 (m, 4H), 2.11−2.02 (m, 2H), 1.87 (app d, 1H), 1.65 (app t, 1H), 1.42 (m, 9H, Me), 1.27 (s, 3H, Me), 1.09 (s, 3H, Me), 0.713 (s, 3H, Me). See also the Supporting Information, Figure S1.

UV−vis spectra and kinetics of slow reactions were recorded with a Shimadzu 3101 PC spectrophotometer at a constant temperature (25 ± 0.2 °C). An Applied Photophysics stopped flow spectrophotometer was used for faster kinetics. Infrared spectra were obtained with a Bio-Rad Digilab FTS-60A FT-IR spectrometer equipped with an MTEC Model 200 photoacoustic cell.[20] NMR spectra were recorded on a Bruker DRX-400 (400 MHz) thermostatted at 298 K. Kinetic analyses were performed with KaleidaGraph 4.03 PC software. Kinetic simulations were carried out with Kinsim/Fitsim Software for PC.[21]

A sky-blue crystal of $[L^2(H_2O)RhNO](ClO_4)_2$ for crystal structure determination was obtained by slow evaporation of a freshly generated solution of $L^2(H_2O)RhNO^{2+}$ in 0.20 M $HClO_4$ under argon. When the crystals of $[L^2(H_2O)RhNO]$-$(ClO_4)_2$ were aged in the mother liquor under air, transparent, needle-shaped crystals formed on the surface of the blue crystals. These were carefully removed and identified as the nitro complex $[L^2(H_2O)RhNO_2](ClO_4)_2$ by crystal structure analysis. An analogous solution that was handled solely under argon also produced crystals of both $[L^2(H_2O)RhNO](OTf)_2$ and $[L^2(H_2O)RhNO_2](OTf)_2$, showing that $L^2(H_2O)RhNO_2{}^{2+}$ is a byproduct in the synthesis of $L^2(H_2O)RhNO^{2+}$, and not the product of autoxidation of the nitrosyl complex. The most likely source of $L^2(H_2O)RhNO_2{}^{2+}$ is the reaction of $L^2(H_2O)$-Rh^{2+} with NO_2, the latter formed by disproportionation of HNO_2[22] which is always present in our solutions of NO.

Results

The crystal structure of *trans*-$[L^2(H_2O)RhNO^{2+}](ClO_4)_2$ (**[1](ClO$_4$)$_2$**) is depicted in Figure 1. The rhodium atom resides at a crystallographic center of symmetry with an

(15) Enemark, J. H.; Feltham, R. D. *Coord. Chem. Rev.* **1974**, *13*, 339–406.
(16) Franke, A.; Hessenauer-Ilicheva, N.; Meyer, D.; Stochel, G.; Woggon, W.-D.; van Eldik, R. *J. Am. Chem. Soc.* **2006**, *128*, 13611–13624.
(17) De, P.; Sarkar, B.; Maji, S.; Das, A. K.; Bulak, E.; Mobin, S. M.; Kaim, W.; Lahiri, G. K. *Eur. J. Inorg. Chem.* **2009**, 2702–2710.
(18) Pestovsky, O.; Bakac, A. *J. Am. Chem. Soc.* **2002**, *124*, 1698–1703.
(19) Bakac, A.; Espenson, J. H. *J. Am. Chem. Soc.* **1988**, *110*, 3453–3457.
(20) Bajic, S. J.; Luo, S.; Jones, R. W.; McClelland, J. F. *Appl. Spectrosc.* **1995**, *49*, 1000–1003.
(21) Barshop, B. A.; Wrenn, R. F.; Frieden, C. *Anal. Biochem.* **1983**, *130*, 134–145.
(22) Pestovsky, O.; Bakac, A. *Inorg. Chem.* **2002**, *41*, 901–905.

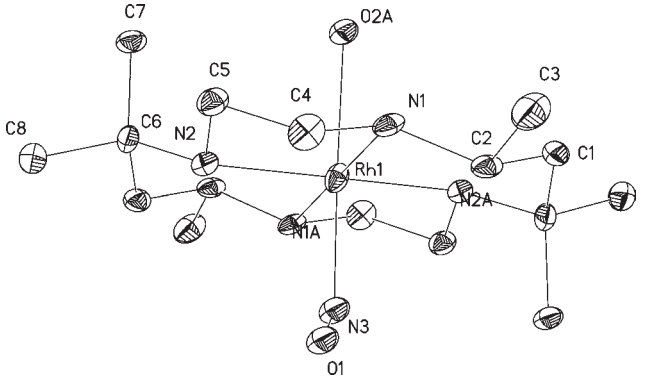

Figure 1. ORTEP drawing of the cation *trans*-$[L^2(H_2O)RhNO]^{2+}$ (**1**) at the 50% probability level. Bond lengths/Å: Rh1−N1(A), 2.083(3); Rh1−N2(A), 2.091(4); Rh1−N3, 1.998(12); Rh1−O2, 2.366(6); N3−O1, 1.19(2). Angles/deg: N1−Rh1−N3, 95.7(5); N1A−Rh1-N3, 84.3(5); N2−Rh1−N3, 87.7(4); N2−Rh1−N3, 92.3(4); Rh1−N3−O1, 122.1(11).

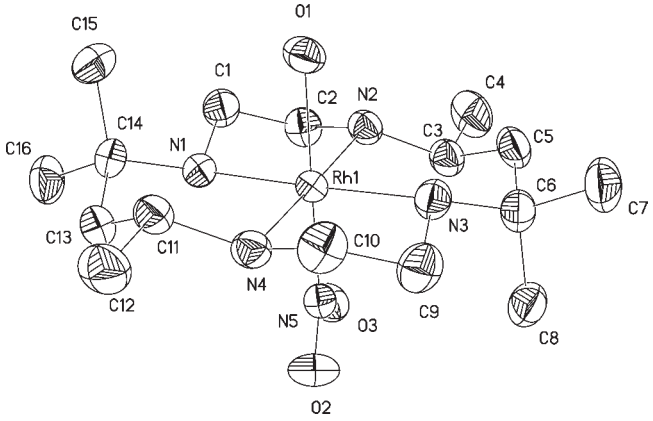

Figure 2. ORTEP drawing of the cation *trans*-$[L^2(H_2O)RhNO_2]^{2+}$ (**2**) at the 50% probability level. Bond lengths/Å: Rh1−N1, 2.098(3); Rh1−N2, 2.075(3); Rh1−N3, 2.078(3); Rh1−N4, 2.074(3); Rh1−N5, 1.988(3); Rh1−O1, 2.124(3); N5−O2, 1.235(4); N5−O3, 1.233(4). Angles/deg: N1−Rh1−N5, 87.47(11); N2−Rh1−N5, 93.99(11); N3−Rh1−N5, 94.28(11); N1−Rh1−N5, 88.03(11); Rh1−N5−O2, 120.8(2); Rh1−N5−O2, 120.0(2).

average equatorial Rh−N bond of 2.087(4) Å and an axial Rh−N(O) distance of 1.998 (12) Å. The short Rh−NO bond and the Rh−N−O angle of 122.1° closely resemble other {M-NO}[8] complexes, such as those of cobalt, iridium and 2-electron reduced {M-NO}[6] compounds of ruthenium and iron.[2,14,23] Also, the long Rh−OH_2 bond (2.366 Å) trans to NO is consistent with the known trans-effect of the reduced nitrosyl ligand.[23,24] These structural parameters are similar to those in the only other reported octahedral {RhNO}[8] complex, $[Rh(MeCN)_3(PPh_3)_2NO]^{2+}$,[25] which has mutually *trans* MeCN ligands and mutually *trans* PPh_3 ligands. The molecular structure shows a Rh−N(O) bond distance of 2.026(8) Å and Rh−NCMe(*trans*) distance of 2.308(3) Å, and a Rh−N−O angle of 118.4 °. For octahedral nitrosyl complexes of the cobalt group metals, molecular orbital theory supports d^6 metal centers when the Rh−N−O angle is 120°.[26,27] The structural parameters for **1** thus strongly support a d^6 Rh, as in the limiting structure $\{Rh^{III}NO^-\}$.[28]

In the nitro complex, $[L^2(H_2O)RhNO_2^{2+}](ClO_4^-)_2\cdot 2H_2O$ ([**2**](**$ClO_4)_2\cdot 2H_2O$**), Figure 2, the Rh−NO_2 bond length (1.988(3)) is comparable to the Rh−NO bond in complex **1**, but the axial Rh−OH_2 bond (2.124 Å) in [**2**] is much shorter than in [**1**], consistent with the lack of a significant trans effect in [**2**]. The four equatorial Rh−N bond distances are comparable for the two complexes and the previously reported $L^2(H_2O)RhOO^{2+}$.[29] The four equatorial nitrogen atoms in [**2**] are planar with a Rms deviation of fitted atoms of 0.0023, and an average equatorial Rh−N bond of 2.081 Å. The Rh atom is displaced from this plane by 0.0337(14)Å.

Aqueous solutions of $L^2(H_2O)RhNO^{2+}$ were quite stable toward dissociation of NO or oxidation with O_2. No decay was observed in Ar- or O_2-saturated solutions in the dark, or in the process of concentrating the preparative solutions by rotary evaporation under reduced pressure.

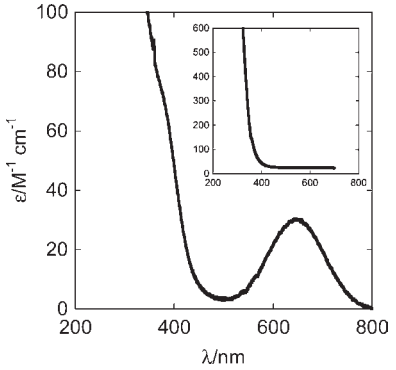

Figure 3. Electronic spectra of $L^2(H_2O)RhNO^{2+}$ (main figure) and $L^2(H_2O)RhNO_2^{2+}$ (inset) in 0.05 M $HClO_4$.

The UV−visible spectrum of the nitrosyl complex exhibits a maximum at 648 nm (ε = 30 M^{-1} cm^{-1}) and a shoulder at 370 nm, as shown in Figure 3. In contrast, the nitro complex has no features in the UV−vis spectrum, but absorbs strongly at λ < 300 nm.

The stoichiometry of the NO/$L^2(H_2O)Rh^{2+}$ reaction, eq 6, was determined by spectrophotometric titration at 648 nm. Spectral changes yielded $[L^2(H_2O)Rh^{2+}]$: NO = 1.0 ± 0.1.

$$L^2(H_2O)Rh^{2+} + NO \longrightarrow L^2(H_2O)RhNO^{2+} \qquad (6)$$

The oxidation of $L^2(H_2O)RhNO^{2+}$ with $Ru(bpy)_3^{3+}$ was monitored at 452 nm, where the product $Ru(bpy)_3^{2+}$ has ε = 1.45× 10^4 M^{-1} cm^{-1}, and at the 650-nm maximum of $L^2(H_2O)RhNO^{2+}$ where $Ru(bpy)_3^{3+}$ also absorbs with ε = 300 M^{-1} cm^{-1}. With $Ru(bpy)_3^{3+}$ in excess over $L^2(H_2O)RhNO^{2+}$, an initial jump in absorbance at 452 nm was followed by a much slower increase, as shown in Figure 4. The overall absorbance change in such experiments yielded a stoichiometric ratio $\Delta[Ru(bpy)_3^{3+}]/\Delta[L^2(H_2O)RhNO^{2+}]$ = 3.6 ± 0.4. The rather large uncertainty is associated with the slow background decomposition of $Ru(bpy)_3^{3+}$ at long reaction times which makes it difficult to establish precisely the end point in the kinetic trace. The overall 4:1 stoichiometry of eq 7 was confirmed independently by detecting close to quantitative yields of nitrate, $[NO_3^-]_\infty/[L^2(H_2O)RhNO^{2+}]_0$ = 0.9, in

(23) Feltham, R. D.; Enemark, J. H. *Topics Stereochem.* **1981**, *12*, 155–215.
(24) Ardon, M.; Cohen, S. *Inorg. Chem.* **1993**, *32*, 3241–3243.
(25) Kelly, B. A.; Welch, A. J.; Woodward, P. *J. Chem. Soc., Dalton Trans.* **1977**, 2237–2242.
(26) Mingos, D. M. P. *Inorg. Chem.* **1973**, *12*, 1209–1211.
(27) Hoffmann, R.; Chen, M. M. L.; Elian, M.; Rossi, A. R.; Mingos, D. M. P. *Inorg. Chem.* **1974**, *13*, 2666–2675.
(28) In the Covalent Bond Classification (CBC), [**1**] is an ML_5X complex, as is $[Rh(MeCN)_3(PPh_3)_2NO]^{2+}$, see: Green, M. L. H. *J. Organomet. Chem.* **1995**, *500*, 127–148.
(29) Bakac, A.; Guzei, I. A. *Inorg. Chem.* **2000**, *39*, 736–740.

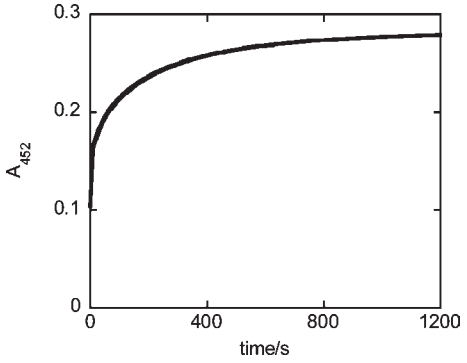

Figure 4. Absorbance changes at 452 nm accompanying the reaction of 4 μM $L^2(H_2O)RhNO^{2+}$ with excess (18 μM) $Ru(bpy)_3^{3+}$ in 1.0 M $HClO_4$.

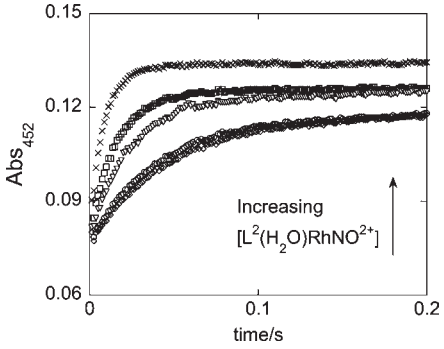

Figure 5. Kinetic traces at 452 nm for the reaction of $Ru(bpy)_3^{3+}$ (4 μM) with excess $L^2(H_2O)RhNO^{2+}$ (86, 114, 200, 285, and 570 μM) in 0.50 M $HClO_4$. All of the traces had the same initial absorbance (0.079).

an experiment that utilized a 5-fold excess of $Ru(bpy)_3^{3+}$ (5×10^{-5} M) over the rhodium complex.

$$L^2(H_2O)RhNO^{2+} + 4Ru(bpy)_3^{3+} + 3H_2O \longrightarrow L^2(H_2O)_2Rh^{3+} + 4Ru(bpy)_3^{2+} + NO_3^- + 4H^+ \quad (7)$$

Under the reverse conditions, that is, with $L^2(H_2O)RhNO^{2+}$ in large excess over $Ru(bpy)_3^{3+}$, only the rapid kinetic step was observed. The total absorbance change in the kinetic traces increased with increasing concentrations of excess reagent, indicative of an equilibrium process. Moreover, the traces exhibit tailing at longer times so that a good fit required a two-term, {exponential + linear} equation. Several representative traces are shown in Figure 5.

The plot of the exponential term against $[L(H_2O)RhNO^{2+}]$, Figure 6, is linear with a slope of $(1.9 \pm 0.1) \times 10^5$ M^{-1} s^{-1} and an intercept of 5 ± 3 s^{-1}.

The data are consistent with a rapid reversible formation of $L^2(H_2O)RhNO^{3+}$, followed by the much slower decomposition, most likely by either homolytic or heterolytic cleavage of the Rh−NO bond, eq 8-9. The follow-up oxidation of the products of reaction 9 leads to additional consumption of $Ru(bpy)_3^{3+}$, eq 10, as established earlier.[12] This chemistry is the source of the slow secondary formation of $Ru(bpy)_3^{2+}$ and of the tailing in the kinetics traces. Another reason for the tailing is the reversibility of reaction 8. In the absence of externally added $Ru(bpy)_3^{2+}$, the importance of the reverse path increases as the reaction progresses and $[Ru(bpy)_3^{2+}]$ builds up, as is clear from the rate law in eq 11.

$$Ru(bpy)_3^{3+} + L^2(H_2O)RhNO^{2+} \rightleftarrows Ru(bpy)_3^{2+} + L^2(H_2O)RhNO^{3+} \qquad k_f,\ k_r,\ K_{Ru} \quad (8)$$

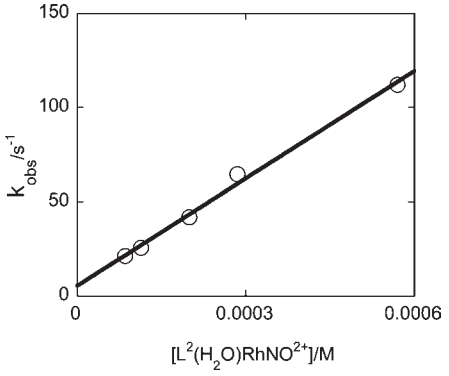

Figure 6. Plot of pseudo-first order rate constants against the concentration of $L^2(H_2O)RhNO^{2+}$ for the reaction with 4 μM $Ru(bpy)_3^{3+}$ in 0.50 M $HClO_4$.

$$L^2(H_2O)RhNO^{3+} \xrightarrow{H_2O} (L^2(H_2O)^2Rh^{3+} + NO) \quad \text{or} \quad (L^2(H_2O)Rh^{2+} + HONO + H^+) \quad (9)$$

$$(L^2(H_2O)_2Rh^{2+}, NO, HONO) \xrightarrow{3Ru(bpy)_3^{3+}} (L^2(H_2O)_2Rh^{3+},\ NO_3^-) \quad (10)$$

$$d[Ru(bpy)_3^{2+}]/dt = k_f[Ru(bpy)_3^{3+}][L^2(H_2O)RhNO^{2+}] - k_r[Ru(bpy)_3^{2+}][L^2(H_2O)RhNO^{3+}] \quad (11)$$

The plot in Figure 6 supports equilibrium kinetics with a dominant forward term. The intercept, 5 s^{-1}, represents the contribution from the reverse reaction. Dividing this value by the concentration of $Ru(bpy)_3^{2+}$ midway through the reaction (ca. 2 μM) yields an estimate for k_r of 3×10^6 M^{-1} s^{-1}.

A more reliable value of this rate constant and of the equilibrium constant K_{Ru} was obtained from the absorbance changes in several experiments, some of which utilized an excess of externally added $Ru(bpy)_3^{2+}$. The $[Ru(bpy)_3^{2+}]_{eq}$ derived from these data was used to calculate the remaining concentrations from the mass balance. These values were substituted into eq 12 to obtain $K_{Ru} = 0.13$ and $k_r = 1.5 \times 10^6$ M^{-1} s^{-1}. The data are summarized in Table 1.

$$K_{Ru} = \frac{k_f}{k_r} = \frac{[Ru(bpy)_3^{2+}]_{eq}[L^2(H_2O)RhNO^{3+}]_{eq}}{[Ru(bpy)_3^{3+}]_{eq}[L^2(H_2O)RhNO^{2+}]_{eq}} \quad (12)$$

One experiment had a large excess of $Ru(bpy)_3^{2+}$ (19 μM) and $L^2(H_2O)RhNO^{2+}$ (150 μM) over $[Ru(bpy)_3^{3+}]$ (6 mM), creating pseudo-first order conditions in both directions and simplifying the kinetic expression to that in eq 13.

$$k_{obs} = k_f[L^2(H_2O)RhNO^{2+}] + k_r[Ru(bpy)_3^{2+}] \quad (13)$$

The fit yielded $k_{obs} = 57$ s^{-1}. After correction for the forward path, that is, $k_f[L^2(H_2O)RhNO^{2+}] = 28.5$ s^{-1}, one calculates $k_r = 1.3 \times 10^6$ M^{-1} s^{-1} (using $[Ru(bpy)_3^{3+}] = 22$ μM at the midpoint of the reaction). This value of k_r agrees well with the average value derived from equilibrium data, 1.5×10^6 M^{-1} s^{-1}, Table 1.

Table 1. Experimental Data Used for Determination of K_{Ru} and k_r

$L^2(H_2O)RhNO^{2+}$/mM	$[Ru(bpy)_3^{3+}]_0/\mu M$	$\Delta[Ru(bpy)_3^{3+}]/\mu M$	$[Ru(bpy)_3^{2+}]_0/\mu M$ (added)	K_{Ru}[a]	k_r[b]/10^6 M^{-1} s^{-1}
0.086	3.5	2.8	0	0.14	1.4
0.11	3.5	2.8	0	0.10	1.9
0.20	3.5	3.0	0	0.09	2.0
0.29	3.5	3.2	0	0.12	1.6
0.15	5.9	4.4	3.4	0.16	1.2
0.15	5.9	3.3	19	0.19	1.0
				0.13 ± 0.04	1.5 ± 0.4

[a] Obtained from equilibrium concentrations and eq 12. [b] Calculated from $k_r = K_{Ru}/k_f$ ($k_f = 1.9 \times 10^5$ M^{-1} s^{-1}).

Table 2. Summary of Rate Constants for the Oxidation of Several Macrocyclic Complexes of Chromium and Rhodium with $Ru(bpy)_3^{3+}$

reductant	k/M^{-1} s^{-1}	source
NO	1.0×10^6	ref 12.
$L^2(H_2O)RhNO^{2+}$	3.1×10^5	this work
$L^2(H_2O)RhOOH^{2+}$	4.7×10^4	ref 13
$L^2(H_2O)RhOO^{2+}$	15.8	ref 13
$L^2(H_2O)RhH^{2+}$	<0.2	ref 13
$L^2(H_2O)CrNO^{2+}$	6.8	ref 13
$L^2(H_2O)CrOO^{2+}$	15	ref 13

The rate constants $k_f = 1.9 \times 10^5$ M^{-1} s^{-1} and $k_r = 1.5 \times 10^6$ M^{-1} s^{-1} were used to simulate the kinetic traces in an effort to obtain the value of the rate constant k_8. These simulations consistently required $k_8 = 0.0093 \pm 0.0001$ s^{-1} for a good fit in 1.0 M $HClO_4$, as shown in the Supporting Information, Figures S3 and S4. At lower acid concentrations, the decay was faster, $k_8 = 0.015$ s^{-1} at 0.50 M H^+, and 0.072 s^{-1} at 0.1 M $HClO_4$, Supporting Information, Figures S5−S6. The ionic strength was not held constant in these experiments and was approximately equal to the concentration of $HClO_4$.

Discussion

Structural and spectroscopic parameters for $L^2(H_2O)RhNO^{2+}$ strongly support a d^6 Rh center, corresponding to the limiting structure $\{(Rh^{III})\text{-}NO^-\}$. Also consistent with a Rh(III) complex is the kinetic stability of complex [**1**] in the absence of added reagents, and the lack of reactivity toward oxygen.

The oxidation of $L^2(H_2O)RhNO^{2+}$ by $Ru(bpy)_3^{3+}$ is remarkable is several respects. The rate constant for initial electron transfer is almost 10^5 times greater than that for the corresponding reaction of the chromium analogue $L^2(H_2O)CrNO^{2+}$ and related chromium complexes. In fact, the oxidation of the rhodium complex is almost as fast as the oxidation of NO itself, which has $k = 1.0 \times 10^6$ M^{-1} s^{-1},[12] Table 2. Moreover, the electron transfer to $Ru(bpy)_3^{3+}$ is reversible and generates a kinetically detectable intermediate with a half-life of about one minute in 1 M $HClO_4$. All of the data strongly suggest that the intermediate is $L^2(H_2O)RhNO^{3+}$, a rare example of a $\{MNO\}^7$ complex of the cobalt group metals. The only other example that we are aware of is $Cl_5Ir^{III}(NO^{\bullet})$, generated recently by electrochemical reduction of $\{Cl_5Ir^{III}(NO^+)\}^6$ at low temperatures.[30,31]

One-electron oxidation of several cobalt[32] and rhodium[33] porphyrin complexes $\{(P)MNO\}^8$ (P = porphyrin, M = Co or Rh) was also reported, but in every instance the oxidation was centered at the porphyrin. Similarly, the coordinated thiolato sulfur was the oxidation site in $\{(N_2S_2)Co(NO)\}^8$ complexes.[34]

The saturated macrocyclic ligand L^2 used in this work is quite resistant to oxidation[35] which makes it an excellent candidate to observe the chemistry centered at the Rh-NO entity. Our assignment of the latter as the site of oxidation by $Ru(bpy)_3^{3+}$ is based on several pieces of evidence. First, the 4:1 stoichiometry and quantitative formation of nitrate, eq 7, rule out oxidation of the macrocycle. That reaction would generate a radical that would almost certainly react either with a second equivalent of $Ru(bpy)_3^{3+}$ or in a disproportionation/dimerization reaction. In both cases the products and stoichiometry would be greatly different from those observed.

The actual value of the rate constant k_f also provides strong support for Rh-NO as the site of oxidation. This value is more than 10^4-fold greater than that for the superoxo complex as shown in Table 2. No such increase was observed in the chromium series where the electronic structure of the metal does not allow for efficient backbonding. In fact, we had concluded earlier that the thermodynamics of electron transfer from superoxo and nitrosyl complexes of chromium had little influence on the kinetics.[13] Clearly, the dramatic change that occurred in the rhodium series must be related to the great difference in electron density and distribution at the metal-NO site. As a result, the oxidation of the nitrosyl complex became so facile that the rate constant exceeds not only that for the oxidation of the superoxo complex, but even that for the hydroperoxo species.

The reversibility of initial electron transfer in reaction 8 makes it possible to calculate the reduction potential for the nitrosylrhodium couple. From $K_{Ru} = 0.13$ and E^0 ($Ru(bpy)_3^{3+/2+}$) = 1.26 V,[36] we obtain E^0 ($L^2(H_2O)RhNO^{3+/2+}$) = 1.31 V, the largest value reported so far for a nitrosyl metal complex, as it exceeds even that of free NO^+/NO ($E^0 = 1.21$ V).[37] The reduction potentials assigned to coordinated NO^+ in iron,[31] ruthenium,[38−40] and osmium[41] complexes cover a

(30) Sieger, M.; Sarkar, B.; Zalis, S.; Fiedler, J.; Escola, N.; Doctorovich, F.; Olabe, J. A.; Kaim, W. *Dalton Trans.* **2004**, 1797–1800.
(31) Doctorovich, F.; di Salvo, F. *Acc. Chem. Res.* **2007**, *40*, 985–993.
(32) Kadish, K. M.; Mu, X. H.; Lin, X. Q. *Inorg. Chem.* **1988**, *27*, 1489–1492.
(33) Wayland, B. B.; Newman, A. R. *Inorg. Chem.* **1981**, *20*, 3093–3097.
(34) Hess, J. L.; Conder, H. L.; Green, K. N.; Darensbourg, M. Y. *Inorg. Chem.* **2008**, *47*, 2056–2063.
(35) Exceptions have been noted, however. The Cr(V) complex, generated by intramolecular electron transfer from coordinated hydroperoxide (Lemma, K.; Ellern, A.; Bakac, A. *Dalton Trans.* **2006**, 58–63) was proposed to decay by intramolecular electron transfer from the ligand.
(36) Creutz, C.; Sutin, N. *Proc. Natl. Acad. Sci. U.S.A.* **1975**, *72*, 2858–2862.
(37) Stanbury, D. M. *Adv. Inorg. Chem.* **1989**, *33*, 69–138.
(38) Chanda, N.; Mobin, S. M.; Puranik, V. G.; Datta, A.; Niemeyer, M.; Lahiri, G. K. *Inorg. Chem.* **2004**, *43*, 1056–1064.
(39) Hadadzadeh, H.; DeRosa, M. C.; Yap, G. P. A.; Rezvani, A. R.; Crutchley, R. J. *Inorg. Chem.* **2002**, *41*, 6521–6526.

range[42] from −0.46 V for $[Os^{II}(CN)_5(NO^+)]^{2-}$ [43,44] to about 0.8 V for several ruthenium polypyridine complexes.[41] The largest reported value for any metal complex prior to this work was 1.19 V for $[Cl_5Ir^{III}(NO^+)]^-$,[31] an $\{IrNO\}^6$ complex that is strongly stabilized by five chloride ligands. Attempts to confirm the oxidation state of NO in $L^2(H_2O)RhNO^{3+/2+}$ by measuring ν_{NO} of this short-lived species have so far been unsuccessful. We are currently exploring new routes to the oxidized complex in hope to generate higher concentrations and to avoid the limitations imposed by intense light absorption by polypyridine ruthenium complexes.

The oxidation product, $L^2(H_2O)RhNO^{3+}$, is itself a powerful oxidant that reacts rapidly with $Ru(bpy)_3^{2+}$. The similar kinetic and thermodynamic data for electron transfer from NO and $L^2(H_2O)RhNO^{2+}$ also require the electron self-exchange rate constant for $L^2(H_2O)RhNO^{3+/2+}$ to be comparable to that for NO^+/NO.

The inverse acid dependence of the kinetics of decay of $L^2(H_2O)RhNO^{3+}$ suggests that the complex participates in an acid−base equilibrium, most likely involving the molecule of coordinated water as in eq 14. In this scenario, the deprotonated form is more reactive, although the implication of this conclusion for the mechanism of the Rh−NO bond cleavage is not totally straightforward. Both homolytic (eq 15) and heterolytic (eq 16) pathways might benefit from decreased acidity, and both would lead to the observed 4:1 stoichiometry for the $Ru(bpy)_3^{3+}/L^2(H_2O)RhNO^{2+}$ reaction.

$$L^2(H_2O)RhNO^{3+} \rightleftarrows L^2(HO)RhNO^{2+} + H^+ \quad (14)$$

$$L^2(HO)RhNO^{2+} \longrightarrow (L^2(HO)Rh^{III})^{2+} + NO \quad (15)$$

$$L^2(HO)RhNO^{2+} + H_2O \longrightarrow (L^2(H_2O)Rh^{II})^{2+} + HNO_2 \quad (16)$$

In summary, an unusual complex with a lifetime of over a minute at pH 0 was generated by oxidation of a novel $\{RhNO\}^8$ cation supported by a robust, saturated N_4 ligand. We expect that the approach adopted in this work will lead to other unusual metal nitrosyls.

Acknowledgment. We are grateful to Dr. Roger Jones for his help in obtaining the photoacoustic spectra, Dr. McClelland for the spectrometer use, and to Dr. Camara and Prof. Rauchfuss for help with solution IR. This work was supported by a grant from National Science Foundation, CHE 0602183. Some of the work was conducted with the use of facilities at the Ames Laboratory.

Supporting Information Available: Crystallographic data for ([**1**]$(ClO_4)_2$) and [**2**]$(ClO_4)_2 \cdot 2H_2O$), Figures S1−S6 and simulation scheme. This material is available free of charge via the Internet at http://pubs.acs.org.

(40) Singh, P.; Das, A. K.; Sarkar, B.; Niemeyer, M.; Roncaroli, F.; Olabe, J. A.; Fiedler, J.; Zalis, S.; Kaim, W. *Inorg. Chem.* **2008**, *47*, 7106–7113.
(41) Pipes, D. W.; Meyer, T. J. *Inorg. Chem.* **1984**, 23.
(42) Roncaroli, F.; Ruggiero, M. E.; Franco, D. W.; Estiu, G. L.; Olabe, J. A. *Inorg. Chem.* **2002**, *41*, 5760–5769.
(43) Baumann, F.; Kaim, W.; Baraldo, L. M.; Slep, L. D.; Olabe, J. A.; Fiedler, J. *Inorg. Chim. Acta* **1999**, *285*, 129–133.
(44) Chanda, N.; Paul, D.; Kar, S.; Mobin, S. M.; Datta, A.; Puranik, V. G.; Rao, K. K.; Lahiri, G. K. *Inorg. Chem.* **2005**, *44*, 3499–3511.